Structural Monitoring and Maintenance, *Vol. 10, No. 3 (2023) 221-242*
https://doi.org/10.12989/smm.2023.10.3.221

Effects of composite and metallic patch on the limit load of pressurized steel pipes elbow with internal defects under opening bending moment

Chaaben Arroussi*[1], Azzedine Belalia[2a] and Mohammed Hadj Meliani[1b]

[1]LPTPM, Departement of Mechanical Engineering, Faculty of Technology, Hassiba BenBouali University of Chlef, P.O. Box. 151 Hay Salem, 02000 Chlef, Algeria
[2]LEM, Faculty of Technology, Hassiba Benbouali University of Chlef, Esalem City, 02000, Chlef, Algeria

(*Received May 30, 2023, Revised September 7, 2023, Accepted September 10, 2023*)

Abstract. Internal and external corrosion are common in pressure pipes used in a variety of industries, often resulting in defects that compromise their integrity. This economically and industrially significant problem calls for both preventive and curative technical solutions to guarantee the reliability of these structures. With this in mind, our study focuses on the influence of composite and metallic patch repairs on the limit loads of pipes, particularly elbows, the critical component of piping systems. To this end, we used the nonlinear extended finite element method (X-FEM) to study elbows, a priori corroded on the internal surface of the extrados section, then repaired with composite and metallic patches. In addition, the effect of the geometry of composite materials and metal patches was examined, in particular the effect of their thickness and material on the increase in limit loads of repaired structures. The results obtained provide information on the effectiveness and optimization of patch repair of corroded elbows, with the aim of increasing their service life.

Keywords: composite patch; critical position; defect; limit load; metallic patch; X-FEM

1. Introduction

Pipelines play an important role in the efficient and reliable transport of hydrocarbons for the regular supply of consumers and industries over vast distances. In these complex networks, elbows are essential components of every piping system, (Firoozabad *et al*. 2016, Muthanna *et al*. 2019).

When contrasted with straight pipes, elbows consider more flexible, allowing them to absorb significant displacements caused by differential thermal or vibratory movements. However, it is important to recognize that potential failures in piping systems frequently originate from the presence of internal or external flaws, part of which is due to corrosion in aggressive environments (Muthanna *et al*. 2019, Boukortt *et al*. 2018, Amara *et al*. 2018). Given these factors, accurate fracture prediction and the preservation of structural integrity within these pipe systems carry considerable significance across diverse practical applications. This is underscored by their

*Corresponding author, Ph.D. Stuedent, E-mail: c.arroussi@univ-chlef.dz
[a]Associate Professor, E-mail: a.belalia@univ-chlef.dz
[b]Professor, E-mail: m.hadjmeliani@univ-chlef.dz

http://www.techno-press.org/?journal=smm&subpage=7 ISSN: 2288-6605 (Print), 2288-6613 (Online)

profound influence on economic considerations and overall security (Li *et al*. 2014, Robertson *et al*. 2005, Balakrishnan *et al*. 2022, Arroussi *et al*. 2022). Furthermore, variations in fluid flow velocity in pipe elbows can lead to turbulence, resulting in vibrations within the elbow component that can lead to its failure (Zhang *et al*. 2015, Meriem-Benziane *et al*. 2021).

According to these issues, extensive studies examined the integrity assessment of pipe elbows using various techniques, including numerical analysis, experimental tests, and analytical approaches for estimating the mechanical integrity of pipeline components (Abbasnia and Shariati 2023, Muthanna *et al*. 2021, Amara *et al*. 2019, Peng and Liu 2019, Duan and Shen 2006).

Numerical tools have been widely used to study various aspects of the elbow corrosion problem in well-defined scenarios of loading, defect profile and extent, and material. These studies, some of which have been validated by experience, have made it possible to simulate the behavior of these critical elements of the piping system, with the aim of gaining a better understanding of the corrosion phenomenon and recommending appropriate solutions. Among others, the following projects are worth mentioning:

Abbasnia and Shariati (2023) investigated the ratcheting behavior on pipe elbow of A234 WPB steel under internal pressure and in-plane cyclic bending. (Subbaiah *et al*. 2022, Salem *et al*.2019, Xie *et al*. 2018, Alexander *et al*. 2009) have focused on analyzing the shapes and positions of defects in the pipe. Duan and Shen (2006) studied the plastic limit pressure of elbows with locally thinned sections located in the extrados. They proposed an empirical formula, which has been experimentally validated. Bruère *et al*. (2019) predicted the failure of a pipe elbow with different idealized defect configurations; they considered internal pressure and axial force. Tee *et al*. (2019) examined the burst strength of a pipe structure containing a single defect, taking into account various geometric parameters of the defect.

On the other hand, the protection of pipeline components has been the subject of careful and diversified studies. However, the use of composite materials is proving more practical in the oil industry, as it is economically advantageous for various forms of defects such as pitting, corrosion, gauge and external corrosion, and can be implemented on in-service pipelines (Prabhakar *et al*. 2109, ASME 2008, Toutanji *et al*. 2001, Alexander *et al*. 2010, Ahmad *et al*. 2022).

Goertzen and Kessler (2007) investigated the mechanical and thermal properties of carbon/epoxy composites used for pipe repair by performing a three-point bending test and examined the effect of heating rate, frequency and measurement method on glass transition temperature. Duell et *al*. (2008) conducted a study in which three-dimensional modeling was used to assess stresses on damaged and repaired carbon/epoxy composite pipes. Their results showed very good agreement with experimental results. Gunaydin *et al.* (2013) studied the influence of glass/epoxy composite patches on the fatigue behavior of notched surface composite pipes. By varying the number of layers, they observed that increasing the number of patch layers improved the fatigue life of repaired pipes.

Meriem-Benziane *et al*. (2015) conducted a comparative analysis of the performance of longitudinal cracks repaired in API X65 pipelines using two different patching methods (single and double patch). Mattos *et al*. (2016) introduced a straightforward approach for obtaining an initial estimation of the burst pressure for a composite repair system used on thin-walled corroded metal pipes. Zhang *et al*. (2020) developed a method to predict the theoretical limit load of composite materials for repairing corroded pipes, along with a refined finite element simulation technique for enhancing structural accuracy. Toudeshky *et al*. (2012) conducted an investigation using the FEM to determine the collapse load of adhesively repaired pipes that contained internal longitudinal defects of varying depths. Gadi *et al*. (2019) explored the use of different composite patches, such

as carbon/epoxy, glass/epoxy, and graphite/epoxy, for repairing cracked bends at a 15° angle. Their analysis primarily focused on calculating the stress intensity factor along the crack using the FEM, aiming to predict crack propagation behavior and implement the repair system in the critical area of the cracked bend. Benyahia *et al*. (2015) demonstrated that the application of composite patches in repairing broken, stressed, bent, or internally pressurized pipes can significantly enhance the lifespan of the repaired pipe.

In fact, the repair methods are diverse, among which another method has been proven to repair damaged pipes by applying a metal patch to the damaged area. This was studied by Cruz *et al*. (2020) on artificially cracked API 5L X52 pipes and repaired using rectangular metal patches bonded with Lord DC-80 adhesive. Repair effectiveness was assessed by visual inspection, incremental pressure tests ranging from 0.68 to 9.8 MPa and strain measurement. The results showed a strong correlation between the experimental tests and the numerical simulations performed using 3D-FEM.

Although elbows are common components used primarily to change flow direction, they are nevertheless the weakest link in piping systems due to their high stress concentration. Obviously, it is often difficult to assess their integrity and resistance to local wall thinning due to corrosion which, accelerated by flow velocity and turbulence, raises serious concerns about the operation, behavior and integrity of these structural elements under service conditions. In response, several studies, both experimental and numerical, have addressed this problem. However, further research is still needed to develop adequate predictive models and to incorporate these models into standards and design codes.

The objective of this study is to investigate defects on the internal surface of a pipe elbow at the extrados section using the extended finite element method (X-FEM). Defects were positioned in three different orientations (0°, 10°, and 45°) and subjected to internal pressure and opening bending moments. Moreover, composite material and metallic patches were used to repair these defects and extend the lifetime of the pipe elbows. Finally, three different types of composite patches were numerically examined.

2. Materials and methods

2.1 Extended Finite Element Method (X-FEM)

In the context of 3D crack modeling using the X-FEM approach for elastoplastic behavior, the displacement field variable $u(x)$ within a cracked field is represented as an extension of the work by Moes *et al.* (1999).

$$u(x) = \sum_{i \in N_{tot}}^{n} N_i(x) u_i + \sum_{i \in N_{saut}} N_i(x) H(x) a_i + \sum_{i \in N_{sing}} N_i(x) \left(\sum_{j=1}^{4} F_j(x) b^j{}_i \right) \tag{1}$$

$N_I(x)$ represents the nodal shape function, u_I represents the nodal displacement vector associated with the continuous part of the solution, H(x) symbolizes the discontinuous jump function that spans across the crack, and a_I signifies the enriched degree of freedom vector within the interior of the crack. The vector bi corresponds to the related nodal enhanced degree of freedom vector at the crack tip. H(x) denotes the Heaviside function, and Fj(x) comprises a set of four specific tip enrichment functions, which can be described as follows

$$Fj\ (x) = r^a\ (2)\ sin\ \frac{\theta}{2}\ ,\quad r^a cos\ \frac{\theta}{2}\ ,\quad r^a sin\ \frac{\theta}{2}\ sin\ \frac{\theta}{2}\ ,\quad r^a cos \frac{\theta}{2} cos\ \frac{\theta}{2} \tag{2}$$

Table 1 Mechanical properties of API X60 pipe steel

Young's modulus, E (GPa)	Poisson's ratio, ν	Yield Strength, σ_y (MPa)	Ultimate Strength, UTS (MPa)
210	0.3	541	588

Table 2 Mechanical properties of composite patch

Young's modulus, E (GPa)			Shear modulus, G (GPa)			Poisson's ratio, ν		
E_{px}	E_{py}	E_{pz}	G_{pxy}	G_{pxz}	G_{pyz}	ν_{pxy}	ν_{pxz}	ν_{pyz}
200	19.6	19.6	7.2	5.5	5.5	0.3	0.28	0.28

Table 3 Mechanical properties of adhesives for patchs

Adhesive (FM73)					Adhesive (DC-80)	
Young's modulus, E_a (GPa)	Poisson's ratio, ν_a	Thermal expansion, (10-6°C)			Young's modulus, E_a (MPa)	Poisson's ratio, ν_a
		α_{12}	α_{12}	α_{12}		
0.42	0.3	4.5	23	23	2383	0.336

Where (r, θ) represent the polar coordinates in the fracture tip's local axis. The exponent value a is 0.5 for linear analysis and $a = 1(1 + n)$ for nonlinear analysis, where n is the strain hardening exponent

The damage parameters in this study are connected to the construction through the application of the X-FEM method for the material used. This method is integrated into the Abaqus computer code (Hollaway *et al*. 2002). The elastic characteristics reported in Tables 1-3 are employed in the subsequent X-FEM analysis. The maximum principal stress equals the nominal strength of 580 MPa. Structural damage occurs due to the initiation and propagation of fractures, leading to separation within the structure. This separation is independent of the mesh architecture. The initiation and propagation of these cracks result in a loss of rigidity, explaining the substantial reduction in the structure's response to loading. However, this phenomenon occurs only after a specific length of propagation relative to the structure's dimensions. This study demonstrates this relationship through load-displacement curves (Bensoltane *et al*. 2023). Numerically, the mesh sections of the structure are assumed to experience damage solely under tension and not under compression, based on the utilized criterion. The criteria for initiating the tensile separation law are as follows (Kim *et al*. 1995)

$$MAXPS = \left\{ \frac{\prec \sigma_{\max} \succ}{\sigma^{o}_{\max}} \right\} = 1 \tag{3}$$

Where $\sigma^{o}_{\max}$ represents the maximum allowable principal stress. The symbol $\prec\succ$ represents the Macaulay bracket with the usual interpretation. the reason for using Macaulay brackets is to indicate that the compressive stress state is not responsible for the onset of damage. the damage begins when the value of the maximum principal stress ratio (Eq. (3)) reaches a value of one (Jing *et al*. 2008).

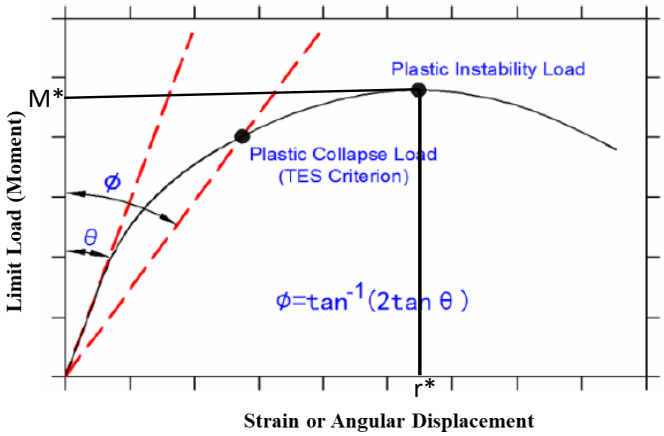

Fig. 1 Determination of the limit load (Lee *et al.* 2015)

2.2 Load limit definition

The term 'limit load' is used in this study to refer to both the instability load and the collapse load. On the load-deflection plot, if the curve approaches a horizontal asymptote, the instability load is referred to as the maximum load.

The collapse load is determined using the "angle method," in which the angle that the linear component of the load-deflection curve makes with the vertical axis is measured, and a line making double this angle with the vertical axis is drawn to intersect the load-deflection curve. The collapse load is the load at the point of intersection (Shalaby and Younan 1998). In this research, our focus is solely on the instability moment as the limit moment under consideration, which corresponds to the maximum moment it can sustain before experiencing structural failure. Fig. 1 represents the method of determining the limit moment.

2.3 Geometrical and materials models

This study aims to demonstrate the effectiveness of composite and metallic patches in enhancing the limit load of pipeline elbows subjected to pressure (P= 9 MPa) and opening bending moment. It also takes into consideration the influence of existing temperature and defects at various critical locations. The geometry used in this investigation is illustrated in Fig. 2, with the outer diameter and wall thickness of the pipe measuring 274 mm and 9.27 mm, respectively. The bend radius of the elbow is R = 381 mm. The selected critical positions for the defect in the elbow are determined based on the study conducted by Arroussi *et al.* (2022), and the dimensions of the defect are a = 4.63 mm and c = 9.27 mm.

The API 5L X60 steel material is utilized to enhance the quality of pipelines, while the composite and metallic patches with layer adhesive technique are used for repairing fractured elbows, the mechanical properties of the pipeline, patch, and adhesive layer are presented in Tables 1-3 respectively. Fig. 3 shows the engineering stress-strain curve for X60 pipeline obtained by Oleg et *al.* (2015).

The pipe elbow is connected to two straight pipes with a length of 600 mm as shown in Fig. 2.

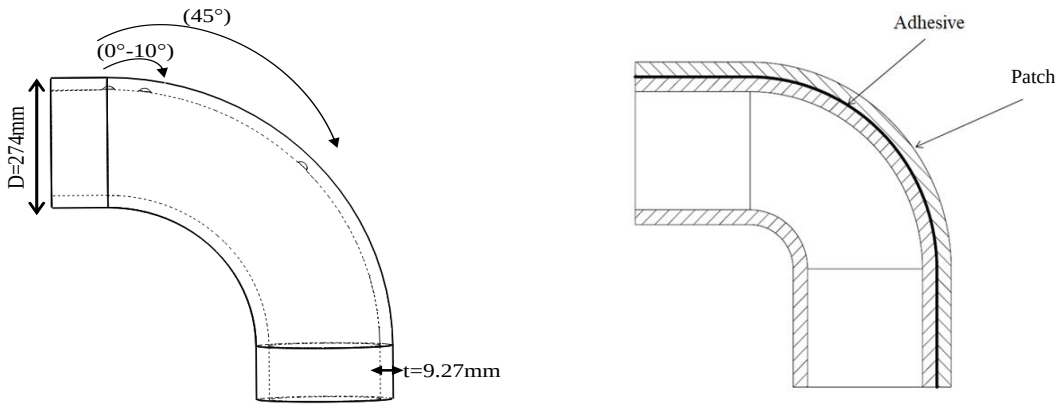

Fig. 2 Geometry of corroded elbow: (a) Critical positions of defect at elbow and (b) Pipe elbow repair by patch

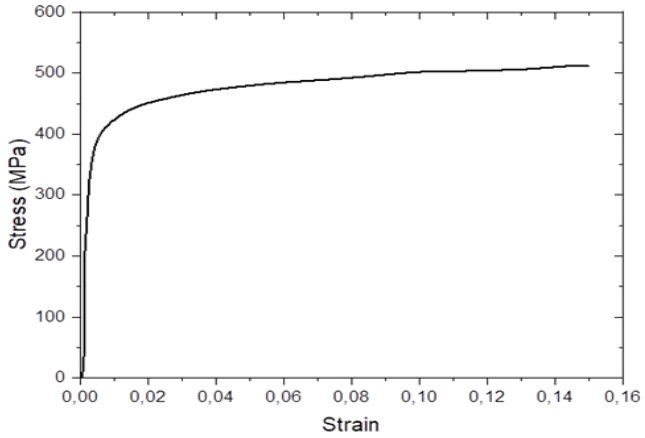

Fig. 3 Nominal stress-engineering strain curve for X60 steel (Oleg *et al*. 2015)

This length is sufficient to ensure that the bend area does not cause stress interference due to the load applied to the end of the linear member. It is assumed that there was no malfunction at the bend. The straight pipe is used solely to uniformly carry the bending moments to the elbow bends. The bending moment load on the elbow was calculated numerically by applying a rotation around the elbow axis.

2.4 Finite element model

In this study, the FE code ABAQUS is used to calculate the limit moment as a function of the end rotation of the pipe elbow. The ends of the pipeline are fixed (Ux, Uy, and Uz = 0) in another linear section of the pipe's edge, while rotation is applied to induce structural damage. The X-FEM is employed to model the cracked pipe elbow, as well as the composite and metallic patch, along

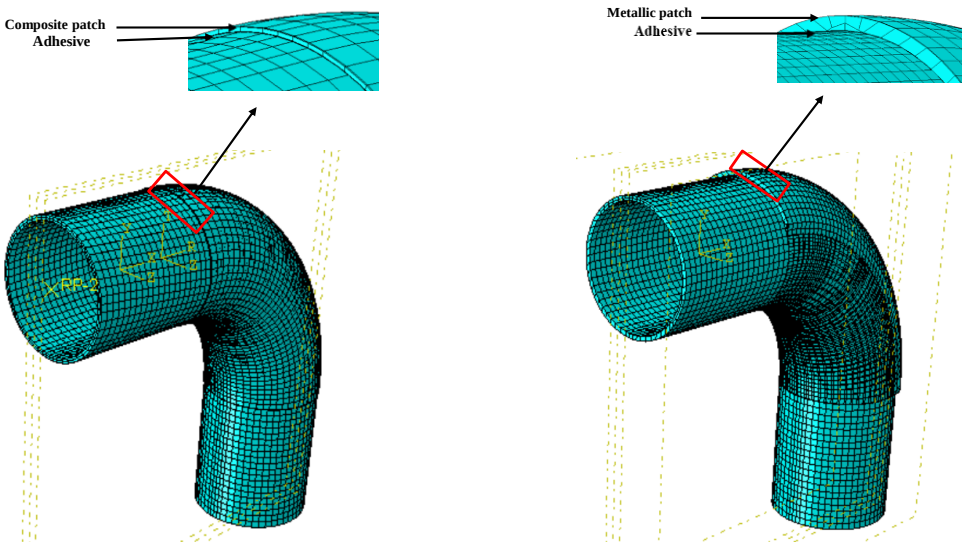

Fig. 4 Mesh view of a defected elbow repaired: (a) Composite patch repair and (b) Metallic patch repair

with the adhesive. It is important to note that the pipe bend is subjected to both pressure and temperature within the tubular structure. The maximum principal stress is determined as equal to the nominal strength value of 580 MPa. The damage assessment criterion is based on the ultimate tensile strength; with a critical crack opening displacement of 1 mm. Three-dimensional hex-dominated quadratic elements are used to create the mesh for the pipe elbow. Fig. 4 illustrates the specimen's mesh and the refined mesh at the fracture tip region.

3. Results and discussion

3.1 Proposal solution

Bonded composite patches are proposed for structural repairs in regions containing internal defects or impacts, aiming to prevent their propagation. In this scenario, the positions are localized within the range of (0° to 45°). The current study focuses on enhancing the strength of the elbow by employing composite patches to delay the occurrence of damage. Optimal patch characteristics, including geometry, number of plies, ply orientations, and structural location, are thoroughly defined to minimize stress concentration in specific areas.

3.2 Effect the number of plies

The composite patch plays a significant role in extending the lifetime of the elbow by increasing the limit moment. As shown in Fig. 5, the composite patch enhances the limit moment by 14%, 30%, and 50% for two, four, and eight composite bondings, respectively, when the defect is located at 0°. Similarly, at a defect position of 10°, the improvement percentages are 10%, 17%, and 64% for two, four, and eight composite bondings, respectively. Furthermore, when the defect

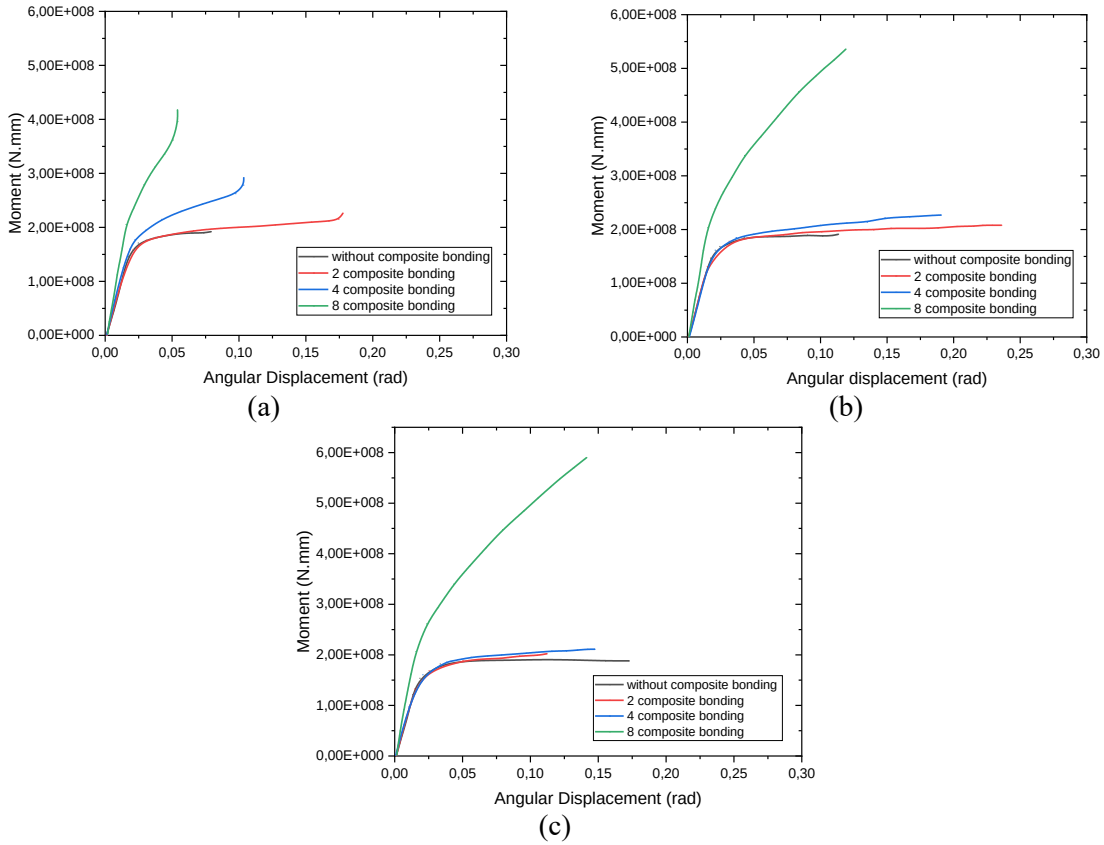

Fig. 5 Bending moment versus angular displacement of elbow repaired by metallic patch (a) position 1 with defect of 0°, (b) position 2 with defect of 10°, and (c) position 3 with defect of 45°

is positioned at 45°, the enhancement percentages are 6%, 11%, and 75% for two, four, and eight composite bondings, respectively.

Additionally, as illustrated in Fig. 5, irrespective of the defect position, it is evident that the limit moment is smallest when utilizing two composite bondings. The utilization of four composite bondings further enhances the limit moment, but the most favorable outcomes are achieved when employing eight composite bondings. Based on the findings of this study, it can be inferred that the most effective approach for enhancing the limit moment of a pipe elbow is the application of eight composite bondings.

This section explores the critical defect positions on the elbow, which range from 0° to 45°. Fig. 6 illustrates the impact of the number of layers (N) in the composite patch on both the limit moment and the corresponding rotation. For a more accurate correlation, we employ the following third-degree equations:

a) Position θ= 0°

$$f(M^*) = 8E+06N^3 - 4E+07N^2 + 8E+07N + 1E+08 \quad (4)$$

$$f(r^*) = 0,0317N^3 - 0,275N^2 + 0,7033N - 0,39 \quad (5)$$

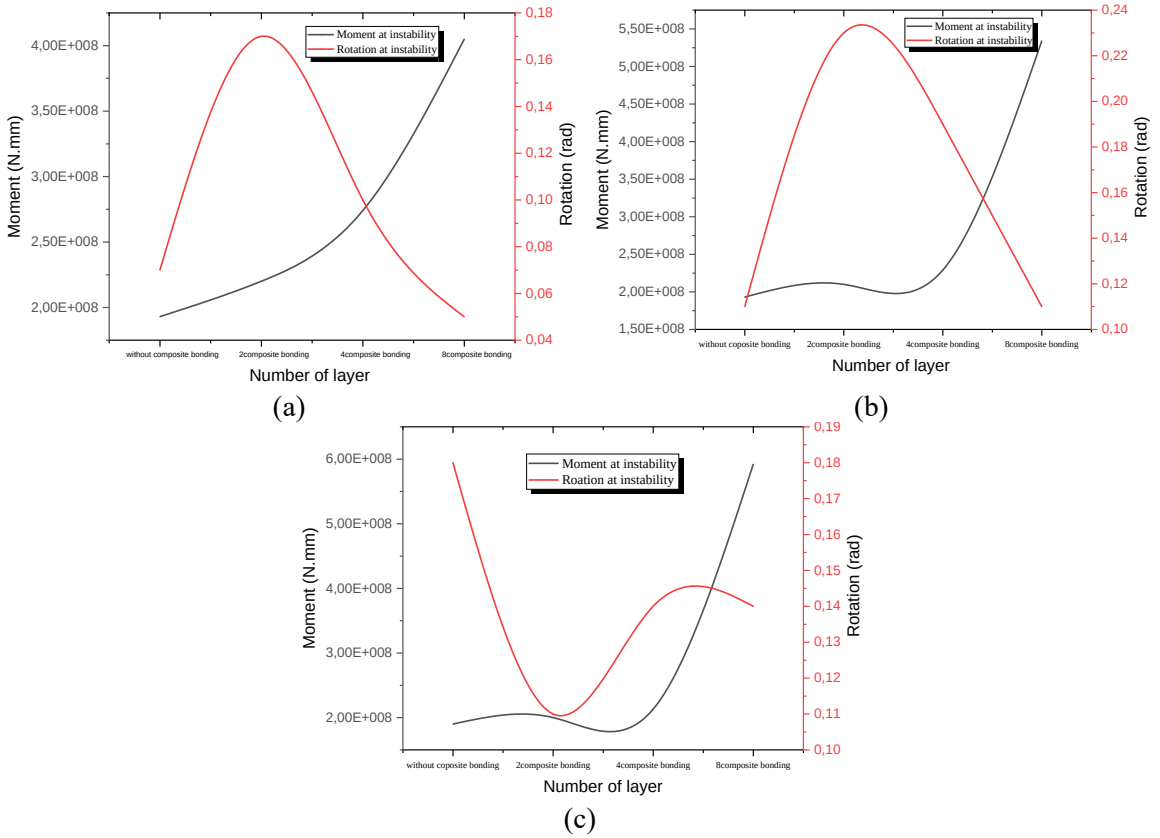

Fig. 6 Rotation-moment versus number of layer for different critical position of defect (a) 0°, (b) 10°, and (c) 45°

b) Position θ=10°

$$f(M^*) = 5E+07N^3 - 3E+08N^2 + 5E+08N - 1E+08 \quad (6)$$

$$f(r^*) = 0,02N^3 - 0,2N^2 + 0,58N - 0,29 \quad (7)$$

c) Position θ=45°

$$f(M^*) = 6E+07N^3 - 4E+08N^2 + 7E+08N - 2E+08 \quad (8)$$

$$f(r^*) = -0,0217N^3 + 0,18N^2 - 0,4583N + 0,48 \quad (9)$$

3.3 Effect of the patch type

The choice of composite reinforcement holds significant importance in material strengthening. Multiple options for reinforcement are available, with the most effective choices being carbon/epoxy, boron/epoxy, and glass epoxy. These materials have showcased superior performance in enhancing the mechanical properties of composite patches.

Table 4 Mechanical properties of three composite patches

	Young's modulus, (GPa)			Shear modulus, (GPa)			Poisson's ratio			Thermal expansion		
	E_1	E_2	E_3	G_{12}	G_{13}	G_{23}	ν_{12}	ν_{13}	ν_{23}	α_{12} (10^{-6})	α_{12} (10^{-6})	α_{12} (10^{-6})
Bore/Epoxy	200	25	25	7.20	5.5	5.5	0.21	0.21	0.21	4.5	23	23
Carbon/Epoxy	112	8.20	8.20	4.5	4.5	4.5	0.3	0.3	0.4	-1.2	34	34
Glasse/Epoxy	50	14.5	14.5	2.56	2.56	2.24	0.33	0.33	0.33	5.5	15	15

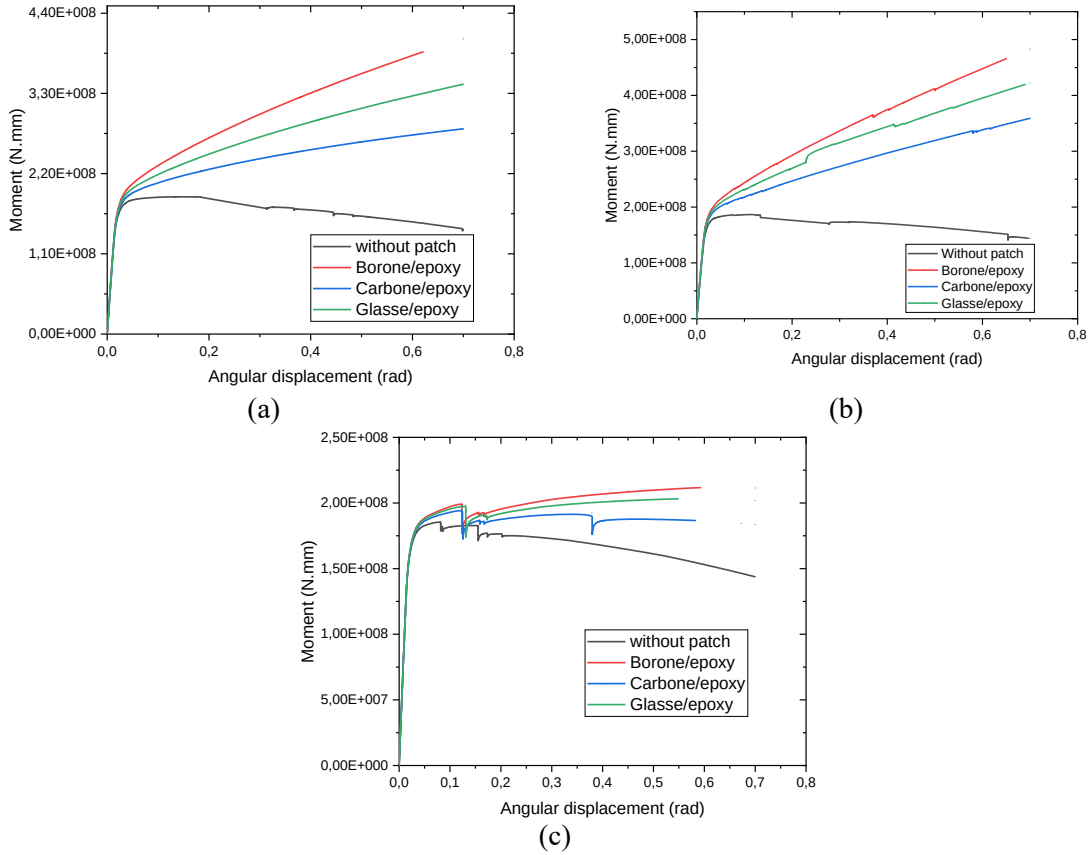

Fig. 7 Moment vs end angular rotation with different types of patch (a) position 1 with defect at 0°, (b) position 2 with defect at 10°, and (c) position 3 with defect at 45°

Table 4 presents the mechanical properties for three types of composite patch. It furnishes detailed insights into crucial attributes like tensile strength, modulus of elasticity, and fracture toughness for each composite material. This data facilitates the evaluation and comparison of performance and suitability among different composite reinforcements for the intended application.

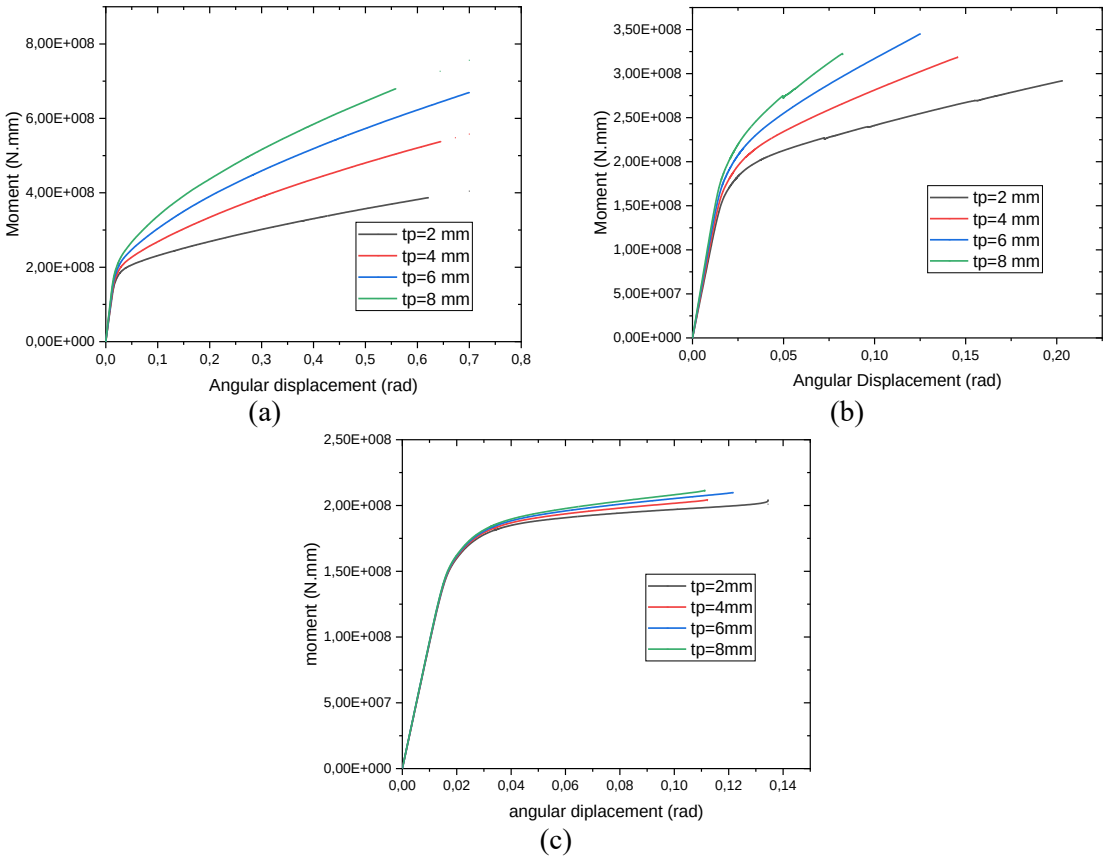

Fig. 8 Moment vs. end rotation angle with different patch thickness. (a) position 1 with defect at 0°, (b) position 2 with defect at 10°, and (c) position 3 with defect at 45°

Fig. 7 highlights the influence of patches in the repair operation, particularly when employing composite materials. The Moment vs. angular displacement at the elbow is crucial for assessing the use of composite patches.

Fig. 7 illustrates the variation in the limit moment of repaired cracked elbows using various composite patch configurations. The choice of composite patch type significantly impacts the moment values. A comparison among the carbon/epoxy, graphite/epoxy, and boron/epoxy patches reveals that the boron/epoxy patch offers superior crack repair performance. The limit moment increases by approximately 59% when the defect position is at 0°, by about 62% when it is at 10°, and by roughly 32% at the 45° position. Based on these findings, the boron/epoxy patch will be utilized in the subsequent numerical analysis.

3.4 Effect of the patch thickness on the elbow failure

Fig. 8 illustrates the influence of composite bonding thickness on the limit moment. The results indicate that the thickness of the composite bonding has a significant impact on the limit moment. As the thickness of the composite bonding increases, the limit moment also increases. For defects

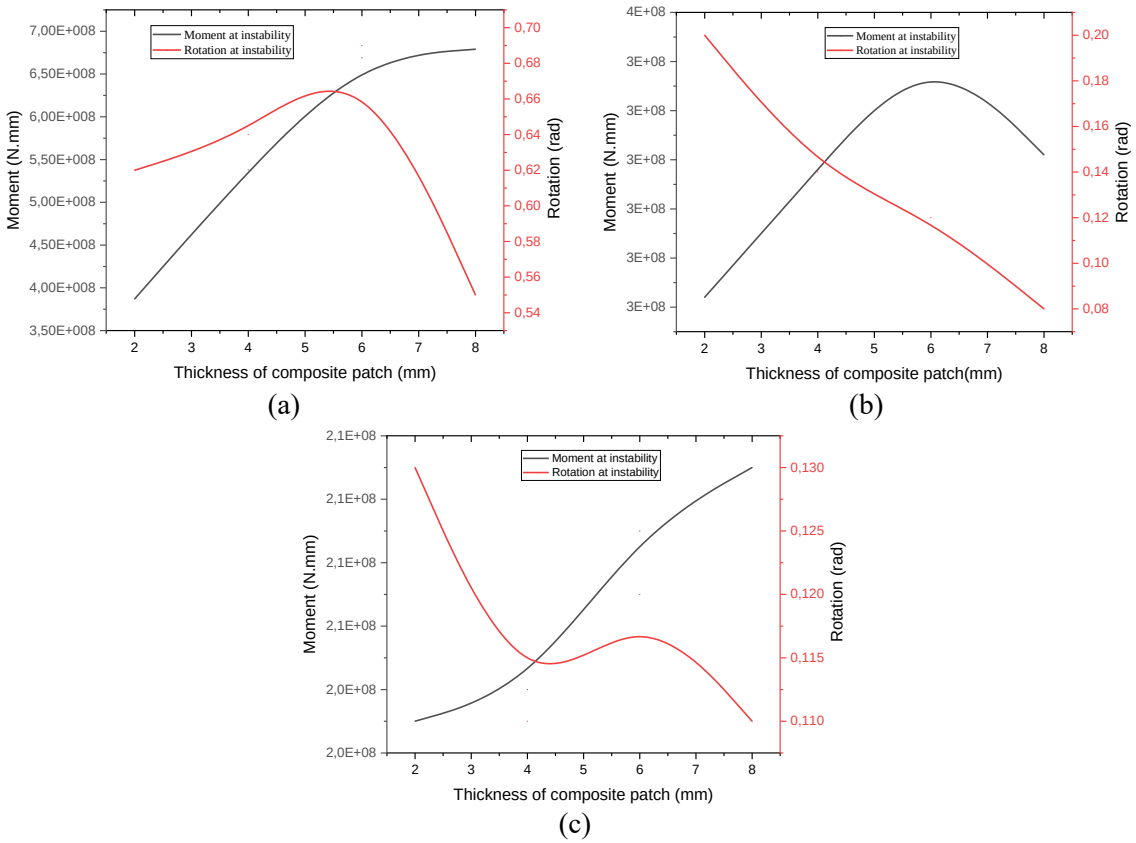

Fig. 9 Rotation-moment versus thickness of composite patch for different critical position of defect (a) 0°, (b) 10°, and (c) 45°

located at 0°, there is an approximate 10% difference in the limit moment. In the case of defects at 10° and 45°, the differences are approximately 50% and 14%, respectively. Based on the analysis of this figure, it can be concluded that an increase in the thickness of the composite wrap leads to an enhancement in the limit moment.

The present section investigates the critical defect position on the elbow, ranging from 0° to 45°. Fig. 9 demonstrates the influence of the composite patch thickness (tp) on the limit moment and the corresponding rotation. To establish a better correlation, a three-degree equation is employed as follows

a) Position θ=0°

$$f(M^*) = -2E+06t_p^3 + 2E+07t_p^2 - 2E+06t_p + 3E+08 \quad (10)$$

$$f(r^*) = -0,0046t_p^3 + 0,0587t_p^2 - 0,2142t_p + 0,85 \quad (11)$$

b) Position θ=10°

$$f(M^*) = -1E+06t_p^3 + 1E+07t_p^2 - 3E+07t_p + 3E+08 \quad (12)$$

$$f(r^*) = -0,0012t_p^3 + 0,02t_p^2 - 0,115t_p + 0,36 \quad (13)$$

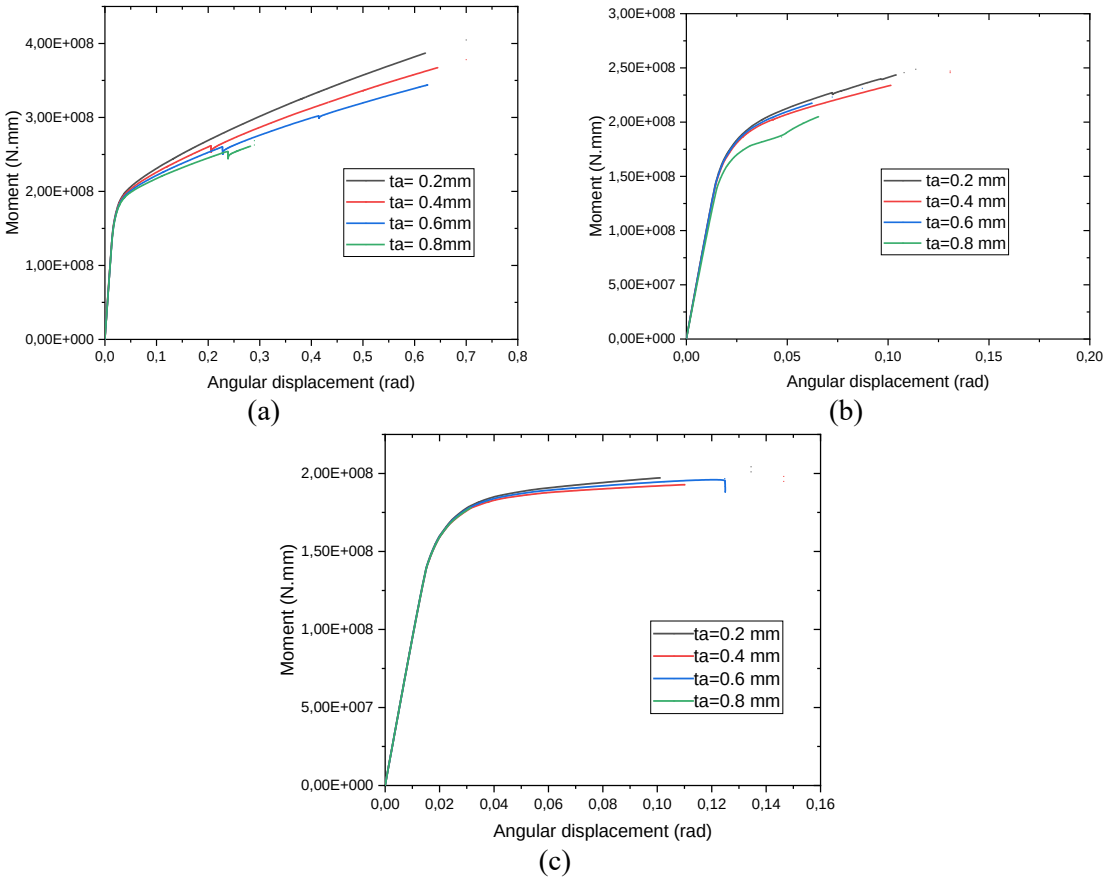

Fig. 10 Moment vs. end rotation angle with different thickness of adhesive (a) position 1 with defect at 0°, (b) position 2 defect at 10°, and (c) position 3 with defect at 45°

c) Position θ=45°

$$f(M^*) = -145833t_p^3 + 2E+06t_p^2 - 9E+06t_p + 2E+08 \quad (14)$$

$$f(r^*) = -0,001t_p^3 + 0,0162t_p^2 - 0,0783t_p + 0,23 \quad (15)$$

3.5 Effect thickness of adhesive

The adhesive layer plays a crucial role in the repair technique of a cracked elbow, as its quality depends on the geometry and material properties. The primary function of the adhesive is to transfer the load from the crack to the composite patch. Fig. 10 depicts the influence of adhesive thickness on the variation of the limit moment of pipe elbows with defects at positions such as 0°, 10°, and 45°. The considered adhesive thicknesses are 0.2, 0.4, 0.6, and 0.8 mm. From Fig. 10, it

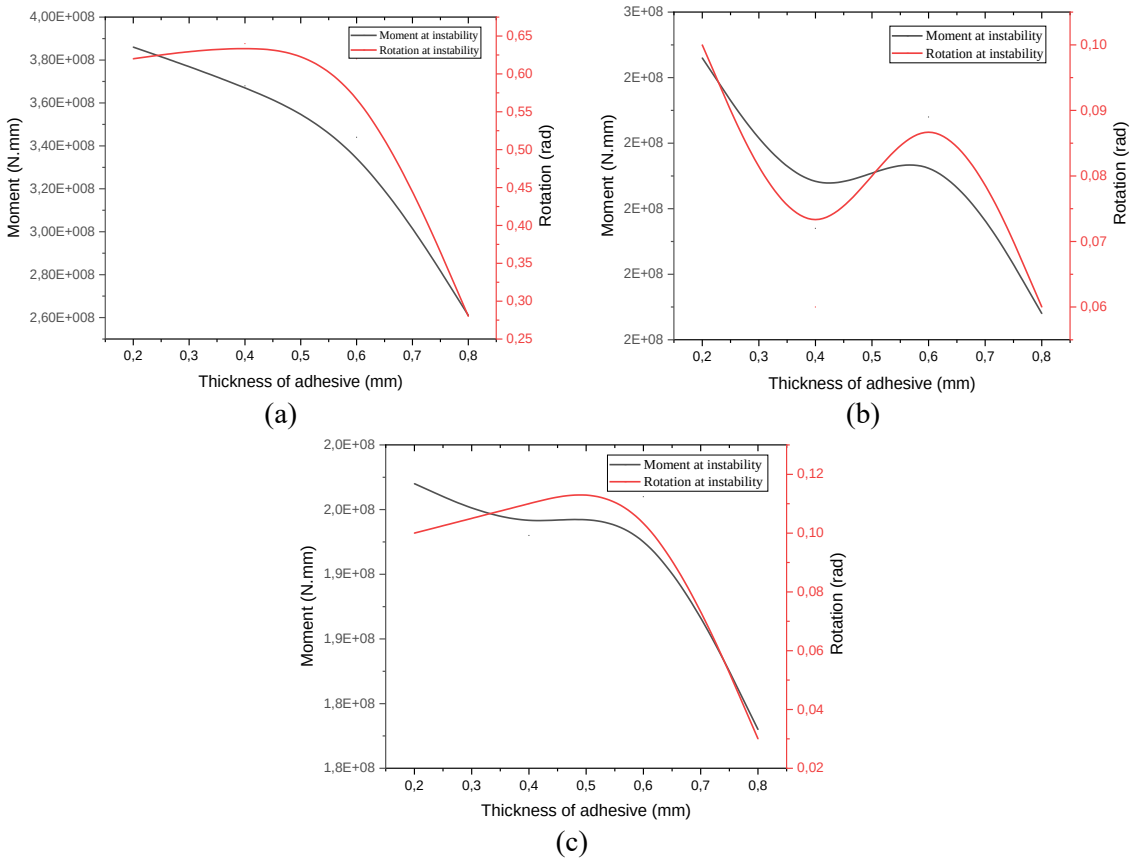

Fig. 11 Rotation-moment versus thickness of adhesive for different critical position of defect (a) 0°, (b) 10°, and (c) 45°

can be observed that reducing the adhesive thickness results in a decrease in the limit moment of the pipe elbow. This decrease indicates that a thinner adhesive facilitates increased load transfer to the composite patch. This section also suggests using thin adhesives for reinforcing damaged specimens.

In this section, the critical position of the defect on the elbow is considered, with values ranging from 0°, 10°, and 45°. Fig. 11 demonstrates that the critical moment and the corresponding rotation are influenced by the thickness of the adhesive (t_a). To establish a better correlation, a three-degree equation is employed, which is presented below

a) Position θ=0°

$$f(M^*) = 1E+09t_a^3 - 2E+09t_a^2 + 1E+09t_a + 7E+07 \quad (16)$$

$$f(r^*) = 5,8333t_a^3 - 11t_a^2 + 6,6667t_a - 0,66 \quad (17)$$

b) Position θ=10°

$$f(M^*) = 2E+09t_a^3 - 3E+09t_a^2 + 1E+09t_a + 4E+07 \quad (18)$$

$$f(r^*) = 3,3333t_a^3 - 5t_a^2 + 2,2667t_a - 0,22 \quad (19)$$

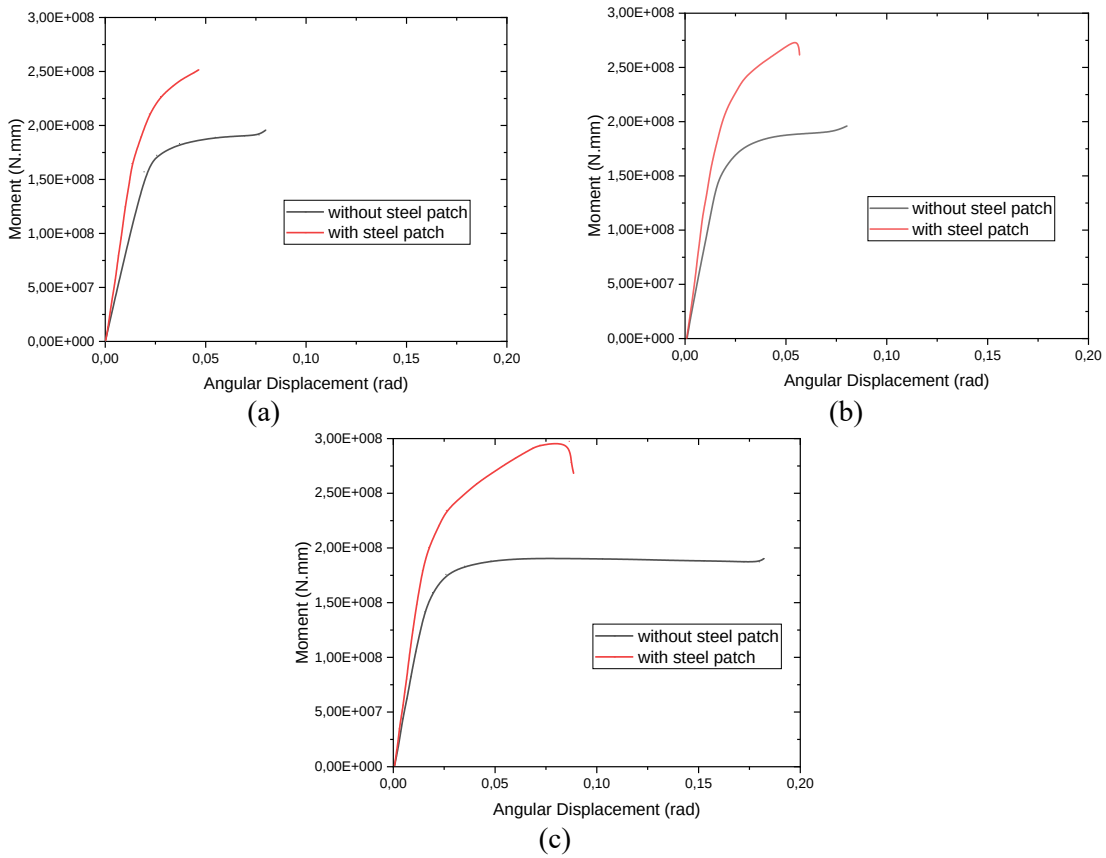

Fig. 12 bending moment versus angular displacement of elbow repaired by metallic patch (a) position 1 with defect at 0°, (b) position 2 defect at 10°, and (c) position 3 with defect at 45°

c) Position θ=45°

$$f(M^*) = -6E+08t_a^3 + 8E+08t_a^2 - 3E+08t_a + 2E+08 \quad (20)$$

$$f(r^*) = -2,0833t_a^3 + 2,5t_a^2 - 0,8667t_a + 0,19 \quad (21)$$

3.6 Metallic patch

More accidents, such as pipeline leakage, are frequently encountered and need to be repaired during service. Pipe leaks are stopped by welding a sleeve-like patch on-site.

3.6.1 The effect of metallic patch on the limit load of cracked pipe elbow

To investigate the effects of a metallic patch on the limit moment of a pipe elbow containing a single defect in three positions (θ=0°, 10°, 45°), Fig. 12 illustrates the variation of the reaction moment versus angular displacement for different elbows with various defect locations. The figure

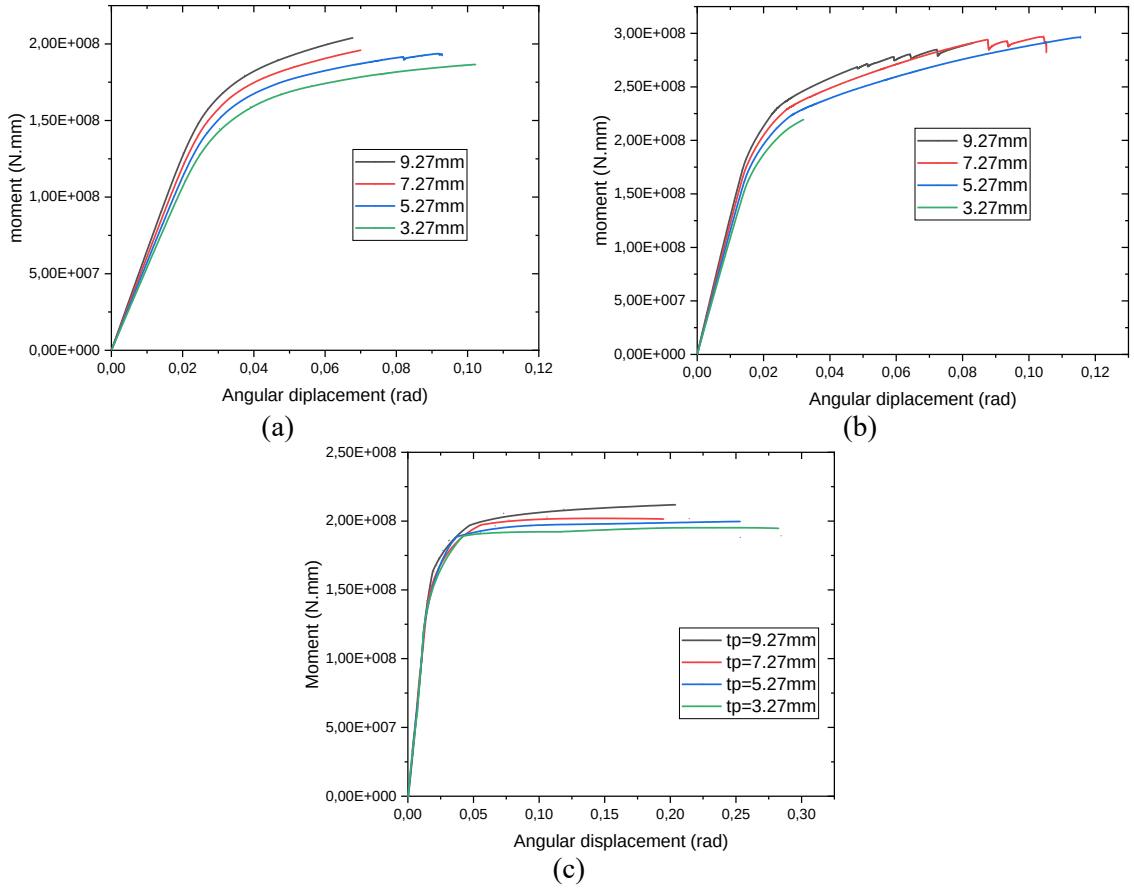

Fig. 13 Moment vs. end rotation angle with different thickness of adhesive.(a) position 1 with defect at 0°, (b) position 2 with defect at 10° and (c) position 3 with defect at of 45°

compares the repaired elbows with metallic patches to the unrepaired pipe elbow. It is evident that the limit moment of the pipe elbow changes considerably when a metallic patch is applied for repair. The metallic patch enhances the limit moment for the elbow by 24% when the defect is located at 0°, 30% when the defect is located at 10°, and 36% when the defect is located at 45°, respectively.

3.6.2 Effect the thickness metallic patch

Fig. 13 illustrates the effect of patch thickness on the limit moment of a pipe elbow with three different defect locations (0°, 10°, and 45°). The figure shows that increasing the patch thickness leads to an increase in the limit moment of the pipe elbow. Specifically, there is a significant increase of approximately 7% when the defect is at 0°, and increases of about 22% and 8% for defect positions of 10° and 45°, respectively. The rate of increase in the critical moment depends not only on the patch thickness but also on its nature, indicating that using a thicker patch enhances its performance.

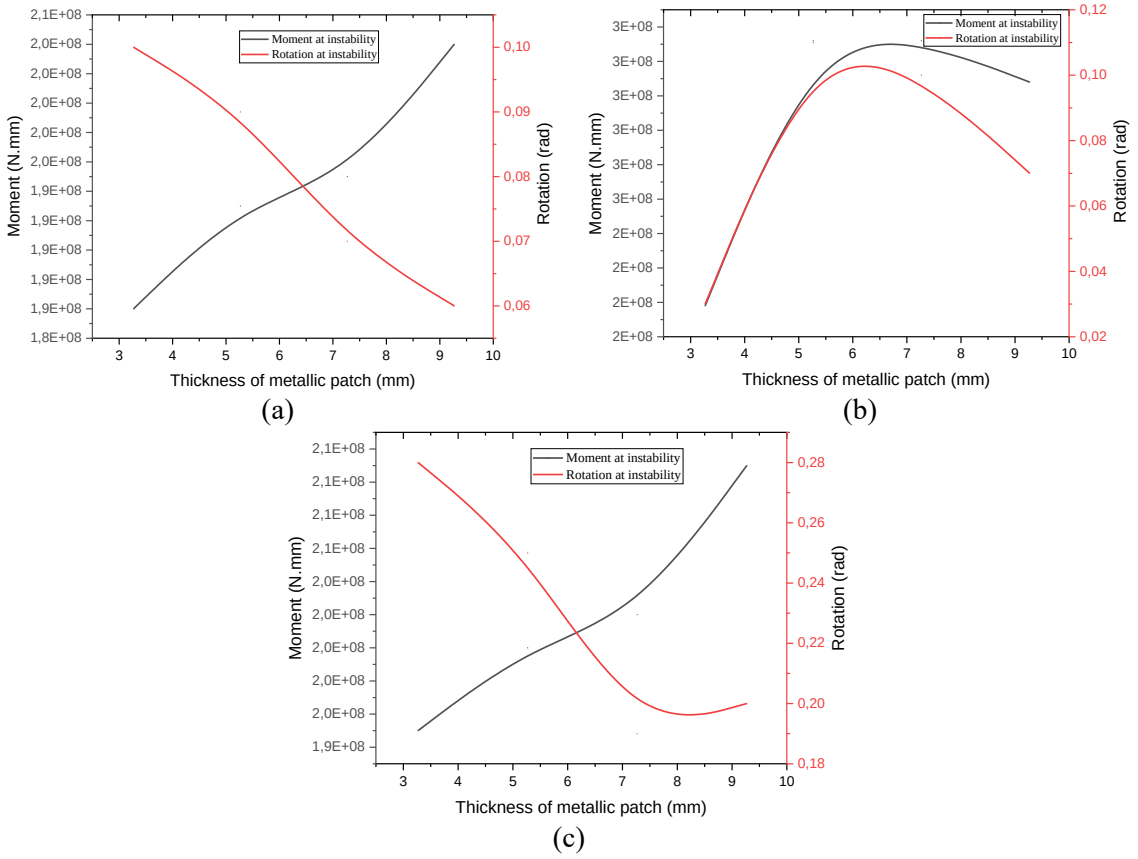

Fig. 14 Rotation-moment versus thickness of metallic patch for different critical position of defect .(a) 0°, (b) 10° and (c) 45°

As indicated by Cruz *et al.* (2020), the repair using a metallic patch demonstrates that the adhesion of the steel patch does not fail and can delay crack propagation without integrity issues, increasing the remaining life of the repaired pipeline across a range of crack sizes, internal pressures, stress distributions, and strain analyses. Adhesive technology is recommended for the convenient and safe repair of API pipelines with various defects, including surface cracks or mild external corrosion. This method is employed in the field of API pipeline repair to ensure their integrity at a reasonable total cost.

The critical position of the defect on the elbow is discussed in this section, considering angles of 0°, 10°, and 45°. As shown in Fig. 14, the limit moment and associated rotation are affected by the thickness of the metallic patch (t_p). To establish a better correlation, a three-degree equation is defined. The equations are as follows

a) Position θ=0°

$$f(M^*) = 250000t_p^3 - 5E+06t_p^2 + 3E+07t_p + 1E+08 \quad (22)$$

$$f(r^*) = 0,0004t_p^3 - 0,0078t_p^2 + 0,0387t_p + 0,0426 \quad (23)$$

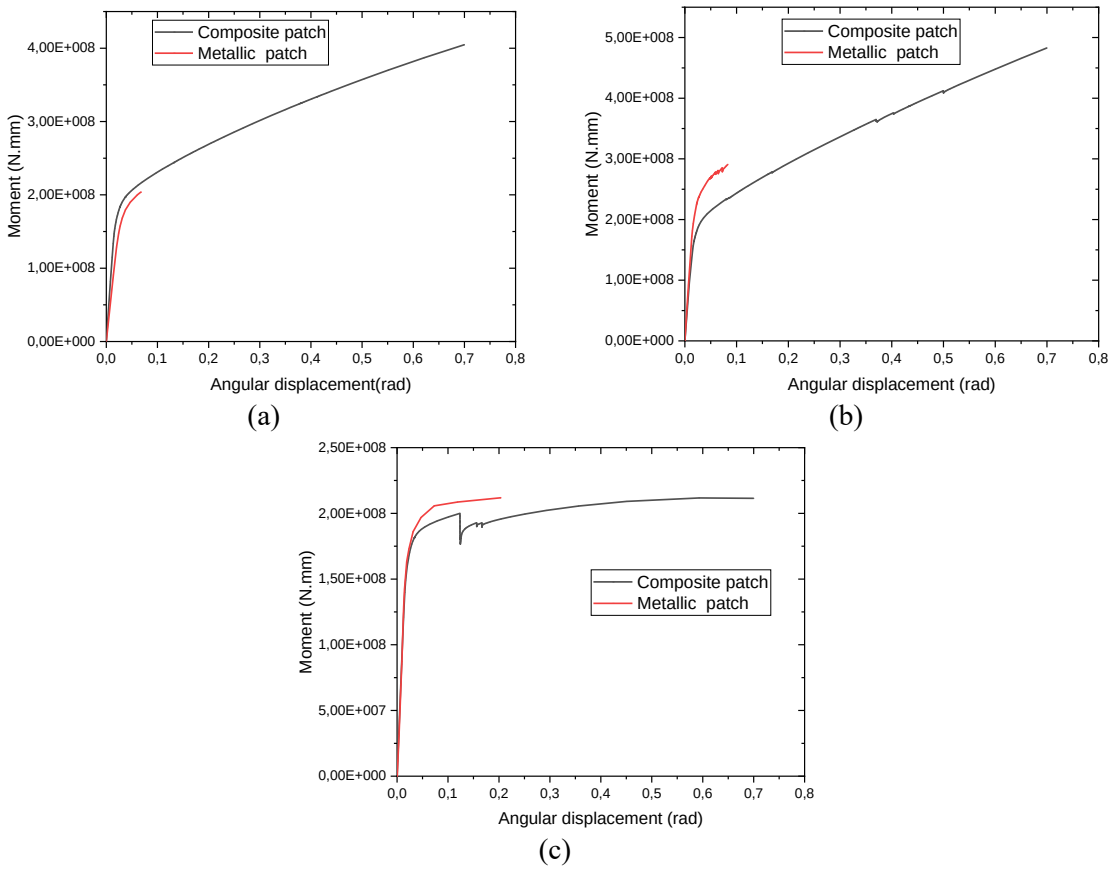

Fig. 15 comparison between repair by composite and metallic patch. (a) position 1 with defect at 0°, (b) position 2 with defect at 10° and (c) position 3 with defect at of 45°

b) Position θ=10°

$$f(M^*) = 1E+06t_p^3 - 3E+07t_p^2 + 2E+08t_p - 2E+08 \quad (24)$$

$$f(r^*) = 0,0015t_p^3 - 0,0343t_p^2 + 0,2517t_p - 0,4774 \quad (25)$$

c) Position θ=45°

$$f(M^*) = 208333t_p^3 - 4E+06t_p^2 + 2E+07t_p + 2E+08 \quad (26)$$

$$f(r^*) = 0,0021t_p^3 - 0,0367t_p^2 + 0,1823t_p + 0,0034 \quad (27)$$

3.7 Comparison between composite patch and metallic patch

In this part of the study, a comparison between the two methods of repairing the damaged elbow by calculating the difference in improvement in the limit load for each case was conducted.

This analysis aimed to determine the better method between the composite patch and metallic patch repair methods.

Fig. 15 illustrates that, in all cases of defect positions, the repair by the composite patch is superior to the metallic patch method. The improvement in the limit load between the two repair methods differs by 49.6%, 39.8%, and 0.4% for the three critical defect positions of 0°, 10°, and 45° respectively. Furthermore, the composite repair exhibits significantly greater displacement values compared to the metallic method, which can be attributed to the superior mechanical properties of the composite material.

4. Conclusions

Various methods exist for repairing defective pipe elbows, involving two types of repairs for damaged pipe elbows: (i) composite bonding and (ii) metallic patching. This analysis employed the X-FEM to compute the limit moment sustained by defective pipe elbows and investigated the enhancement of the limit moment after repair. The key research findings were as follows: The repaired pipe elbow exhibited an improved critical moment compared to the unrepaired pipe. The defect's position significantly influenced the repair's effectiveness, with the critical moment being smallest when employing two composite bondings. When the defect was at 0°, using four composite bondings yielded a higher enhancement of the critical moment compared to other positions. The most effective method for enhancing the pipe elbow's critical moment was repairing it with eight composite bondings. The metallic patch repair method significantly enhanced the pipe elbow's critical moment for various defect positions.

In direct comparison, the study concluded that using a composite patch for repair was superior to using a metallic patch in enhancing the pipe elbow's critical moment. These findings offer valuable insights into the efficacy of distinct repair methods, accounting for defect position and material selection. They suggest that employing multiple composite bondings and patches can substantially improve the repaired pipe elbow's limit moment, surpassing the performance of the metallic patch repair method.

References

Abbasnia, S.K. and Shariati, M. (2023), "Experimental and numerical investigation of ratcheting behavior in seamless carbon steel 90° elbow pipe with small dimensions under constant internal pressure and in-plane cyclic bending", *Int. J. Press. Vessels Pip*, **204**, 104974. https://doi.org/10.1016/j.ijpvp.2023.104974.

Ahmad, H., Ejaz, M.F. and Aslam, M. (2022), "Nonlinear numerical analysis and proposed equation for axial loading capacity of concrete filled steel tube column with initial imperfection", *Struct. Monit. Maint.*, **9**(1), 81-105. https://doi.org/10.12989/smm.2022.9.1.081.

Ahmed-Bensoltane, A., Mokhtari, M., Benzaama, H., Samet, K., Benrouba, H. and Abdelouahed, E (2023), "Using XFEM technique to pPredict the effect of default on the damage of steel pipe Reduced-connection under bending and pressure loading", *Int. J. Steel Struct.*, **23**(1), 316-330. https://doi.org/10.1007/s13296-022-00697-w.

Alexander, C. and Ochoa, O. (2010), "Extending onshore pipeline repair to offshore steel risers with carbon–fiber reinforced composites", *Compos. Struct.*, **92**(2), 499-507. https://doi.org/10.1016/j.compstruct.2009.08.034

Alexander, C.R. (2009) "Evaluating damaged subsea pipelines using an engineering-based integrity management program", *In ASME International Offshore Pipeline Forum*, Houston, TX, ASME Paper No. IOPF2009-6002.

Amara, M., Muthanna, B.G.N., Abbes, M.T. and Meliani, M.H. (2018), "Effect of sand particles on the Erosion-corrosion for a different locations of carbon steel pipe elbow,", *Procedia Struct. Integr.*, **13**, 2137-2142. https://doi.org/10.1016/j.prostr.2018.12.151.

Arroussi, C., Mouna, A., Meliani, M.H. and Pluvinage, G (2022), "Proposal engineering methods to repair/replace bend elbow pipe contain internal corrosion defect", *Procedia Struct. Integr.*, **41**, 752-758. https://doi.org/10.1016/j.prostr.2022.05.087.

ASME (2008), "Repair of pressure equipment and piping," *American Society of Mechanical Engineers*, New York, Standard No. PCC-2.

Balakrishnan, S., Veerappan, A.R. and Shanmugam, S. (2022), "Development of a new improved closed-form plastic collapse moment solution for structurally distorted and through-wall axially cracked 90° pipe bends subjected to in-plane closing bending moment", *Int. J. Press. Vessels Pip.*, **199**, 104736. https://doi.org/10.1016/j.ijpvp.2022.104736.

Benyahia, F., Albedah, A., Bachir Bouiadjra, B. and Belhouari, M. (2015), "A comparison study of bonded composite repairs of through-wall cracks in pipes subjected to traction, bending moment and internal pressure", *Adv. Mater. Res.*, **1105**, 41-45. doi:10.4028/www.scientific.net/AMR.1105.41.

Boukortt, H., Amara, M., Meliani, M.H., Bouledroua, O., Muthanna, B.G.N., Suleiman, R.K., Sorour, A.A., Pluvinage, G. (2018), "Hydrogen embrittlement effect on the structural integrity of API 5L X52 steel pipeline", *Int. J. Hydrogen. Energ.*, **43**(42), 19615-19624. https://doi.org/10.1016/j.ijhydene.2018.08.149.

Bruère, V.M., Bouchonneau, N., Motta, R.S., Afonso, S.M.B., Willmersdorf, R.B., Lyra, P.R.M., Torres, J.V.S., de Andrade, E.Q. and Cunha, D.J.S. (2019), "Failure pressure prediction of corroded pipes under combined internal pressure and axial compressive force Cunha", *J. Braz. Soc. Mech. Sci. Eng.*, **41**(172). https://doi.org/10.1007/s40430-019-1674-2.

Cruz, C., Vargas, B., Capula, S., Terán, G., Guzmán, I. and Granda, E. (2020), "Experimental and finite element analysis of a damaged API5L X52 pipeline with longitudinal crack repaired by adhesively bonded metallic patch", *J. Adhes. Sci. Technol.*, **35**(11), 1170-1184. https://doi.org/10.1080/01694243.2020.1838109.

Da Costa Mattos, H.S., Reis, J.M.L., Paim, L.M., Da Silva, M.L., Junior, R.L. and Perrut, V.A. (2016), "Failure analysis of corroded pipelines reinforced with composite repair systems", *Eng. Fail. Anal.*, **59**, 223-236. https://doi.org/10.1016/j.engfailanal.2015.10.007

Duan, Z.X. and Shen, S.M (2006), "Analysis and experiments on the plastic limit pressure of elbows", *Int. J. Press. Vessels Pip.*, **83**(10), 707-713. https://doi.org/10.1016/j.ijpvp.2006.08.003.

Duell, J.M., Wilson, J.M. and Kessler, M.R. (2008), "Analysis of a carbon composite overwrap pipeline repair system", *Int. J. Press. Vessels Pip.*, **85**(11),782-788. https://doi.org/10.1016/j.ijpvp.2008.08.001.

Firoozabad, E.S., Jeon, B.G., Choi, H.S. and Kim, N.S. (2016), "Failure criterion for steel pipe elbows under cyclic loading", *Eng. Fail. Anal.*, **66**, 515-525. https://doi.org/10.1016/j.engfailanal.2016.05.012.

Gadi, I., Meriem-Benziane, M. and Bouiadjra, B.B. (2019), "Finite element method investigation of geometrical influences of adhesive and patch in the safety for 90° elbow piping system", *J. Mech. Eng. Sci.*, **13**(4), 5973-5987. https://doi.org/10.15282/jmes.13.4.2019.17.0473.

Goertzen, W.K. and Kessler, M.R. (2007), "Dynamic mechanical analysis of carbon/epoxy composites for structural pipeline repair", *Compos. B. Eng.*, **38**(1), 1-9. https://doi.org/10.1016/j.compositesb.2006.06.002.

Gunaydin, B., Daghan, B. and Avci, A. (2013), "Fatigue behavior of surface-notched composite pipes repaired by composite patches", *Int. J. Damage Mech.*, **22**(4), 490-498. http://dx.doi.org/10.1177/1056789512450596.

Hollaway, L. and Cadei, J. (2002), "Progress in the technique of upgrading metallic structures with advanced polymer composites", *Prog. Struct. Eng. Mater.*, **4**(2), 131-148. https://doi.org/10.1002/pse.112.

Hosseini-Toudeshky, H. and Fadaei, E. (2012), "Effects of composite patch geometry on collapse load of pressurized steel pipes with internal longitudinal flaws", *Appl. Mech. Mater.*, **152**, 381-386.

Jing, J., Gao, F., Johnson, J., Liang, F.Z., Williams, R.L. and Qu, J. (2008), "Simulation of dynamic fracture along solder-pad interfaces using a cohesive zone model", *Int. Mech. Eng. Congress Expo.*, **48678**, 171-176. https://doi.org/10.1115/IMECE2008-68891.

Kim, J.K., Kim, D.S. and Takeda, N. (1995), "Notched strength and fracture criterion in fabric composite plates containing a circular hole", *J. Compos. Mater.*, **29**(7), 982-998. https://doi.org/10.1177/002199839502900706.

Lee, G.H., Pouraria, H., Seo, J.K. and Paik, J.K. (2015), "Burst strength behaviour of an aging subsea gas pipeline elbow in different external and internal corrosion-damaged positions", *Int. J. Nav. Archit.*, **7**(3), 435-451. https://doi.org/10.1515/ijnaoe-2015-0031.

Li, J., Zhou, C.Y., Xue, J.L. and He, X.H. (2014), "Limit loads for pipe bends under combined pressure and out-of-plane bending moment based on finite element analysis", *Int. J. Mech. Sci.*, **88**, 100-109. https://doi.org/10.1016/j.ijmecsci.2014.07.012.

Lyapin, A.A., Chebakov, M.I., Dumitrescu, A. and Zecheru, G. (2015), "Finite-element modeling of a damaged pipeline repaired using the wrap of a composite material", *Mech. Compos. Mater.*, **51**(3), 1-8. https://doi.org/10.1007/s11029-015-9504-9.

Meriem-Benziane, M., Abdul-Wahab, S.A., Zahloul, H., Babaziane, B., Hadj-Meliani, M. and Pluvinage, G. (2015), "Finite element analysis of the integrity of an API X65 pipeline with a longitudinal crack repaired with single- and double-bonded composites", *Compos. B. Eng.*, 77, 431-439. https://doi.org/10.1016/j.compositesb.2015.03.008.

Meriem-Benziane, M., Bou-Said, B., Muthanna, B.G.N. and Boudissa, I. (2021), "Numerical study of elbow corrosion in the presence of sodium chloride, calcium chloride, naphthenic acids, and sulfur in crude oil", *J. Pet. Sci. Eng.*, **198**, 108124. https://doi.org/10.1016/j.petrol.2020.108124.

Moës N., Dolbow, J. and Belytschko, T. (1999), "A finite element method for crack growth without remeshing", *Int. J. Numer. Meth. Eng.*, **46**(1), 131-150. https://doi.org/10.1002/(SICI)1097-0207(19990910)46:1<131::AID-NME726>3.0.CO;2-J.

Muthanna, B.G.N., Amara, M., Meliani, M.H., Mettai, B., Božić, Ž., Suleiman, R. and Sorour, A.A. (2019), "Inspection of internal erosion-corrosion of elbow pipe in the desalination station", *Eng. Fail. Anal.*, **102**, 293-302. https://doi.org/10.1016/j.engfailanal.2019.04.062.

Muthanna, B.G.N., Bouledroua, O., Meriem-Benziane, M., Hadj-Meliani, M., Pluvinage, G. and Suleiman, R.K. (2019), "Numerical study of semi-elliptical cracks in the critical position of pipe elbow", *Frat. ed Integrita Strutt.*, **13**(49), 463-477. https://doi.org/10.3221/IGF-ESIS.49.44.

Muthanna, B.G.N., Bouledroua, O., Meriem-Benziane, M., Setvati, M.R. and Djukic, M.B. (2021), "Assessment of corroded API 5L X52 pipe elbow using a modified failure assessment diagram", *Int. J. Press. Vessels Pip.*, **190**, 104291. https://doi.org/10.1016/j.ijpvp.2020.104291.

Peng, H. and Liu, Y. (2019), "Shakedown and limit analysis of 45-degree piping elbows under internal pressure and cyclic in-plane bending", *PVP – ASME*, **58967**, V005T09A003. https://doi.org/10.1115/PVP2019-93263.

Prabhakar, M.M., Rajini, N., Ayrilmis, N., Mayandi, K., Siengchin S., Senthilkumar, K., Karthikeyan, S. and Ismail, S.O. (2019), "An overview of burst, buckling, durability and corrosion analysis of lightweight FRP composite pipes and their applicability", *Compos. Struct.*, **230**. https://doi.org/10.1016/j.compstruct.2019.111419.

Robertson, A., Li, H. and Mackenzie, D. (2005), "Plastic collapse of pipe bends under combined internal pressure and in-plane bending", *Int. J. Press. Vessels Pip*, **82**(5), 407-416. https://doi.org/10.1016/j.ijpvp.2004.09.005.

Salem, M., Mechab, B., Berrahou, M., Bachir Bouiadjra, B. and Serier, B. (2019), "Failure analyses of propagation of cracks in repaired pipe under internal pressure", *J. Fail. Anal. Prev.*, **19**(1), 212-218. https://doi.org/10.1007/s11668-019-00592-3.

Shalaby, M.A. and Younan, M.Y. (1997), "Limit loads for pipe elbows with internal pressure under in-plane closing bending moments", *Am. Soc. Mech. Eng. Press. Vessels Pip. Div. (Publ.) PVP*, **347**, 203-213. https://doi.org/10.1115/1.2841882.

Subbaiah, A. and Bollineni, R. (2020), "Stress intensity factor of inclined internal edge crack in cylindrical pressure vessel", *J. Fail. Anal. Prev.*, **20**, 1524-1533. https://doi.org/10.1007/s11668-020-00948-0.

Tee, K.F. and Wordu, A.H. (2019), "Burst strength analysis of pressurized steel pipelines with corrosion and gouge defects", *Eng. Fail. Anal.*, **108**. https://doi.org/10.1016/j.engfailanal. 104347.

Toutanji, H. and Dempsey, S (2001), "Stress modeling of pipelines strengthened with advanced composites materials", *Thin-Walled Struct.*, **39**(2), 153-165. https://doi.org/10.1016/S0263-8231(00)00049-5.

Trifonov, O.V. (2015), "Numerical stress-strain analysis of buried steel pipelines crossing active strike-slip faults with an emphasis on fault modeling aspects", *J. Pipeline Syst. Eng. Pract.*, https://doi.org/10.1061/(ASCE)PS.1949-1204.0000177.

Xie, M. and Tian, Z. (2018), "A review on pipeline integrity management utilizing in-line inspection data", *Eng. Fail. Anal.*, **92**, 222-239. https://doi.org/10.1016/j.engfailanal.2018.05.010

Zhang, T., Zhang, Y.O. and Ouyang, H. (2015), "Structural vibration and fluid-borne noise induced by turbulent flow through a 90 piping elbow with/without a guide vane", *Int. J. Press. Vessels Pip.*, **125**, 66-77. https://doi.org/10.1016/j.ijpvp.2014.09.004.

Zhang, Y., Cheng, Z. and Jia, Z. (2022), "Failure loads analysis of corroded pipe repaired by composite material under tension and internal pressure", *J. Mar. Eng. Technol.*, **21**(3), 178-188. https://doi.org/10.1080/20464177.2020.1826675.

JK